Cold Season's Air Temperature Geostatistical Modeling: Considering the Landsat Thermal Band and Snow Cover Area

Masoud Minaei[a1]

[a] *Assistant Professor, Department of Geography, Ferdowsi University of Mashhad, Mashhad, Iran.*

Received: 12 February 2017
Accepted: 2 October 2017

Abstract

Providing climatic data like temperature in good spatial resolution is a key requirement for many geographical, ecological and bioclimatic research. With this in mind, various related studies use thermal remote sensing images as auxiliary data to enhance the air temperature interpolation outcomes. That while normally summer season images are used as auxiliary data and less attention has been paid to winter season acquired images which are often covered by snowy areas. With this in mind, the Snow Covered Area (SCA) extent impacts on air temperature interpolation were investigated. The data used were temperature data and four Landsat thermal images of December 1986 and 1999. To calculate the area of snow cover, band combination and NDSI index were used. Results show that Thermal Co-Kriging (TCK) of December 1986 provide better results with more snow affected thermal image. While in 1999 although different results were obtained but the best selected output did not show impacts of different snow cover area. These results revealed that probably the SCA extent threshold could be different and could be found with more research. Finally, we know that number of our observation stations are too low and considering the Kriging requirements like normal distribution and stationarity are toilsome but we should consider that this problem exists in the regions with low density of gauges and should find a way to enhance the air temperature interpolation in these cases. At the end, using high resolution, Landsat thermal bands improve our ability to explain and visualize local temperature variability into a variety of applications such as deriving temperature dependent climatic variables, species distribution modelling and assessments of fire risk.

Key words: Interpolation, Thermal co-kriging, Kriging, Golestan

1. Introduction

Spatial interpolation is one of the most often-used geographic techniques for spatial data visualization, spatial query of properties, and spatial decision-making processes in geography, earth sciences, and environmental science (Meng, Liu and Borders, 2013).

1 Corresponding author: Masoud Minaei. Tel: +989355471477 E-mail: m.minaei@um.ac.ir

Indeed, spatial interpolation is often used to predict a value of a variable of interest at unmeasured locations with available measurements at sampled sites (Kyriakidis and Goodchild, 2006; Meng et al., 2013). Moreover, the spatial interpolation also applies for temperature mapping. Air temperature is one of the input variables for land evaluation and characterization systems, as well as hydrological and ecological models (Benavides, Montes, Rubio and Osoro, 2007; Minaei and Irannezhad, 2016). Benavides et al. (2007) and some others (e.g,. Li, Cheng, and Lu, 2005) believe that air temperature modeling in mountainous regions is a challenge and it is dififcult to obtain precise climatic maps
Nonetheless, different interpolation methods have been used to model the spatial distribution of air temperature. The most widely used are the inverse distance interpolation weighting, Voronoi tessellation, regression analysis or, more recently, geostatistical methods (Benavides et al., 2007; Minaei and Minaei, 2017; Moteallemi, Bina, Minaei and Mortezaie, 2017). The addition of auxiliary variables is often believed to increase the performance of spatial prediction (Meng et al., 2013). Some auxiliary variables that are used whole around the world by researchers in different fields of study are Digital Elevation Model (DEM), slope, aspect, distance to sea, solar radiation, land cover, NDVI and so on (Benavides et al., 2007; Boi, Fiori and Canu, 2011; Jabot, Zin, Lebel, Gautheron and Obled, 2012; Meng, 2006). For example, Kalivas, Kollias and Apostolidis, (2013) applied the slope as the auxiliary data to interpolate the forest volume as an interesting topic for forest managers. Alsamamra, Ruiz-Arias, Pozo-Vazquez and Tovar-Pescador, (2009) interpolated the solar radiation in the southern Spain and used elevation and shadows cast as external variables. Meng (2014) used IKONOS bands 2 and 3 which was auxiliary data to interpolate band 2 using regression kriging versus Geographically Weighted Regression method.
In case of temperature interpolation using auxiliary data, Boi et al. (2011) used five parameters including elevation, sea distance, longitude, latitude and relative elevation to interpolate means of maximum and minimum daily temperatures. Meng et al. (2013) investigated the spatial interpolation of annual maximum temperature in the central Big Sur in California using elevation as the auxiliary variable. Benavides et al., (2007) implemented geostatistical modeling over a mountainous region in the Spain to interpolate monthly mean air temperature and used the elevation as an auxiliary data. Arundel (2005) included elevation and slope as independent variables to interpolate the temperature and precipitation. Hengl, Heuvelink, Tadic, and Pebesma, (2012) used latitude, longitude, DEM, topographically weighted distance from the coast line, and topographic wetness index, total insolation and MODIS LST images to provide daily temperature maps. They found that MODIS time series of LST images could be successfully combined with ground measurements of temperatures to produce more accurate and more detailed predictions of daily temperature (Hengl et al., 2012). A problem in their study was regarding the MODIS images that had 10-30% missing pixels. Cristobal, Ninyerola and Pons, (2008) measured the role of geographical and remotely sensed predictors in air temperature interpolation in the Catalonia, Spain. They used altitude, latitude, continentality and solar radiation as geographical variables and LST and NDVI in Landsat TM, ETM+, AVHRR and MODIS images. They identify that combined geographical and remotely sensed variables provide better results and among these

variables the LST and NDVI are the most powerful remote sensing predictors. Zheng, Zhu and Yan, (2013) performed monthly air temperature interpolation using MODIS LST and NDVI, too. Stewart and Nitschke (2017) recently used MODIS LST and local topography to improve temperature interpolation.

Literature reveals that remotely sensed data can provide a valuable source of information to understand spatial phenomena (Joyce, Wright, Samsonov and Ambrosia, 2009) and are able to deal with the thermal characteristics of earth surface (Prakash, 2000). Most of the studies, however, used warm season acquired RS images as auxiliary data. While we want to investigate the usability of cold season remote sensing images as auxiliary data because we need accurate spatial temperature data in all seasons. In case of cold season images, in the north east of Iran as like as many areas in high latitudes, ground surface of satellite images acquired in cold seasons (if the sky be cloud free) are covered by snow. According to the snow cover area (SCA) the impact on the air temperature and dependency of thermal data s nature to temperature we decided to use the snow covered thermal images in spatial interpolation. We aimed to investigate the relationship between the area of snow covered lands and accuracy of interpolation.

To this end, we decided to use thermal band of Landsat because of better resolution in comparison to MODIS to answer the requirement of many geographical, ecological, biological, and bioclimatic spatial studies to higher resolution information in their studies (Attorre, Alfo, De Sanctis, Francesconi, and Bruno, 2007; Zaksek and Schroedter-Homscheidt, 2009); however, these have not been thoroughly tested to date. In this regard, to analyze the impact of area of snow cover in providing spatial data of temperature, we used four approximately cloud free Landsat thermal images, two for December 1986 and two others for December 1999 to evaluate SCA and temperature interpolation relationships in a complex topographic region of north-east of Iran. In other words, this research will investigate the relations between the extent of snow cover area in the thermal remote sensing images as auxiliary data and spatial interpolation of mean air temperature using Geostatistics.

Study area

Study area is located in the northeastern part of Iran and covers an area of 18000 km^2 (Fig. 1). It is located between the latitude of 36ذ 43 and 38ذ 07 N and the longitude of 54ذ 19 and 56ذ 25 E. It included most of Gorganrood watershed and parts of Atrak and Gharasoo watersheds. The altitude range is between -30 to 2956 meters above sea level. This region is very important from a number of viewpoints. First, its agricultural production activities are important, as it has valuable and fertile soils. Second, about 2,000,000 people live in flood prone areas within the study zone (Statistical-Center-of-Iran, 2012). Third, Golestan National Park, a UNESCO heritage site, is located in this region, and contains valuable and old forests, a high level of diversity in terms of flora and fauna, as well as a number of endangered species, all of which suffer when there are floods, Climate Change (CC) and Land Cover/Land Use change (LCLUc) (Minaei and Kainz, 2016). Moreover, the study area is a geographically complex region that experiences remarkable climate variations. The plains are located in the east and center, while to the south the area is covered by dense forests and dry highlands. The northern

area is semi-arid and mostly hilly in terms of its topography (Delbari, Afrasiab and jahani, 2013; Minaei and Minaei, 2017).

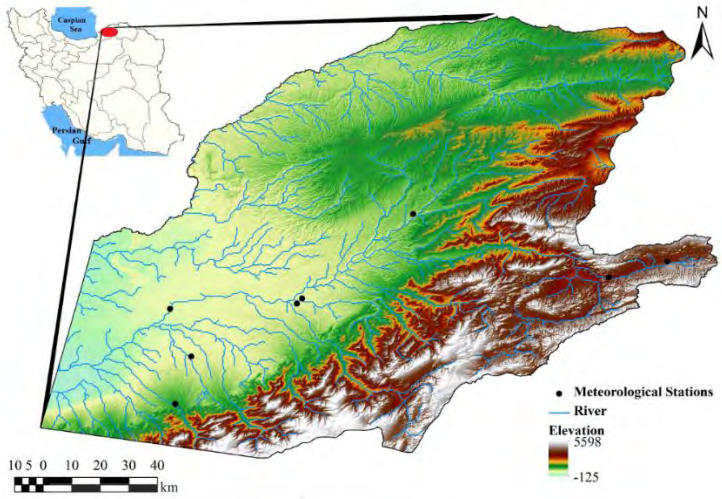

Fig 1. Location of study area and meteorological stations

Materials and Methods

This research will follow the methodology flowchart presented in the Fig. 2. The air temperature data will be interpolated using thermal images as auxiliary and simultaneously the SCA of images will be extracted by NDSI index to be used in analyzing the results. Detailed description of methodology is presented below.

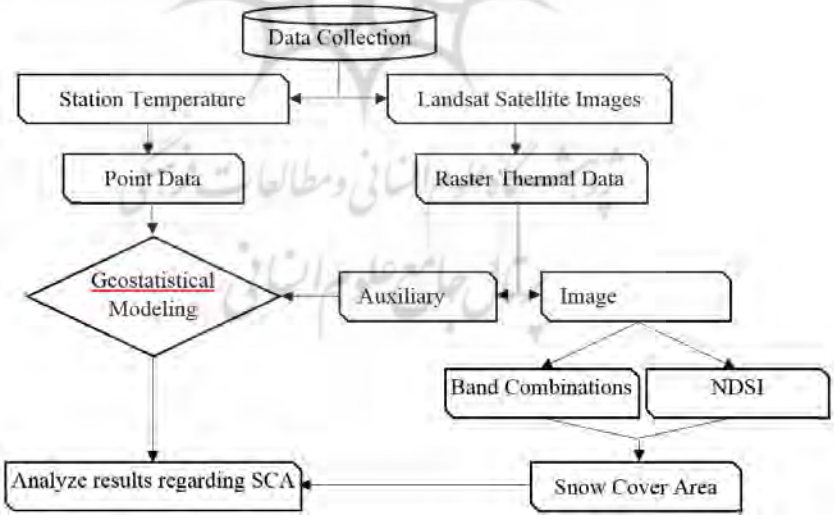

Fig. 2. Methodology Flowchart

For this research, two categories of data were used: mean air temperature data (Table 1) as station points and Remote Sensing images as raster. Thermal bands of four approximately cloud free Landsat TM and ETM+ images (path 162, row 34) for

December 1986 and 1999 were the raster data of the research (Fig. 3). TM and ETM+ sensor thermal bands are in the 10.40-12.50 µm with spatial resolution of 120/60 m (USGS, 2013). The images from EROS Data Center have already been processed into a standard level of geometric and terrain accuracy (Minaei and Minaei, 2017). Therefore, images were selected and downloaded from the United States Geological Surveys (USGS) National Center for Earth Resources Observation and Science (http://glovis.usgs.gov).

Table 1. Meteorological Stations

Station	Latitude	Longitude	Elevation(m)
Tamar	37° 29	55° 30	132
Gonbad	37° 14	55° 09	36
Araz-kuse	37° 13	55° 08	34
Bhalke Dashli	37° 04	54° 47	24
Fazel-abad	37° 54	54° 45	210
Sad-gorgan	37° 12	54° 44	12
Ghafar-haji	37° 00	54° 08	-22
Cheshme-khan	37° 18	56° 07	1250
Robat-gharabil	37° 21	56° 18	1450

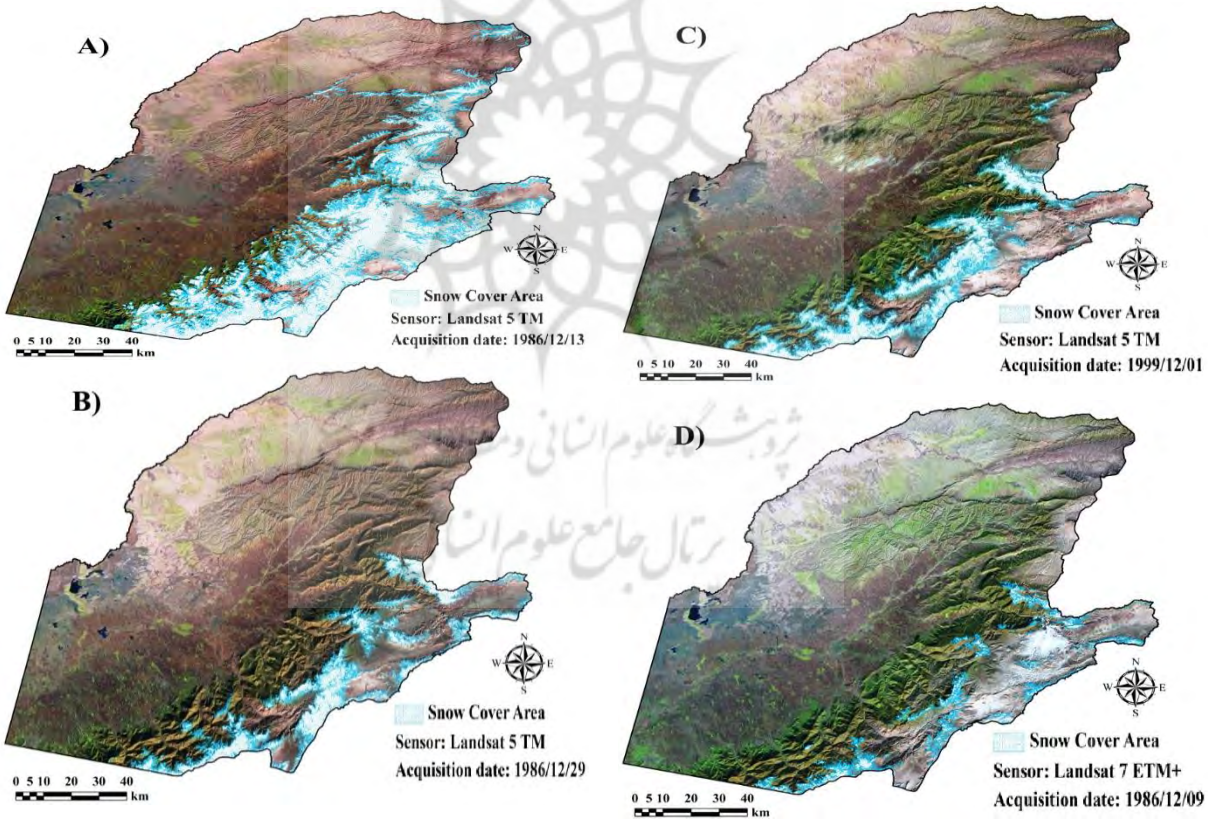

Fig. 3. Satellite images of the study area with SCA in A) 1986 first image (3786.9 Km^2), B) 1986 second image (1003 Km^2), C) 1999 first image (1261.4 Km^2) and D) 1999 second image (367.2 Km^2)

Geostatistics: Kriging/Co-Kriging

As a brief description, Kriging is a geostatistical interpolation method derived from regionalized variable theory. It assumes that the distance, direction or both can be employed to explain variation in the surface between observations that show spatial correlation (Chen, Yue, Dai and Tian, 2013). Kriging can offer the best linear unbiased estimates with an accurate description of the spatial structure of the data and valuable information about estimation error distributions (Chen et al., 2013; Oliver and Webster, 1990). A clear improvement to ordinary space˚ time kriging includes the use of auxiliary data to aid the estimation process, referred to as external drift (Wentz, Peuquet, and Anderson, 2010). Co-kriging is a versatile statistical approach for spatial point estimation, especially, when both primary and auxiliary attributes are available. If each component of $z(s_0)$ satisifes the intrinsic hypothesis that assumes that stationarity of the differences. between pairs of data points exists in the ifrst and . econd moments, then Co-kriging is unbiased and deifned by equations 1, 2, and . (Meng, 2006; Meng et al., 2013).

$$\hat{z}(s_0) = \sum_{j=1}^{n} z(s_j)\Lambda_{j\bullet} \quad (1)$$

$$\sum_{j=1}^{n} \Lambda_{j\bullet} = I \quad (2)$$

$$\sum_{\emptyset=1}^{v} \Gamma(s_i,s_j) + \Psi = \Gamma(s_i,s_0) \quad i = 1, \dots, n \quad (3)$$

Where I is an identity matrix = $[1, 0, \dots, 0]^T$, T indicates a transpose, and $\Lambda_{j\bullet}$ is the weights associated with the prediction. $z(s_j)$ is the vector $z_1(s_j) \dots z_m(s_j)$. $\Gamma(s_i,s_j)$ and $\Gamma(s_i,s_0)$ are the cross variograms and Ψ is the Lagrange Multiplier for i from 1 to n (Meng, 2006; Meng et al., 2013). We used the original thermal bands of Landsat and not the LST or NDVI as the auxiliary data to reduce the input data preparing time and to provide a bigger range of values in the predictor variable. At the end, the ordinary and simple kriging and Co-kriging with and without transformations (regarding season data properties), optimization and stable model were implemented and tested and the results of them were compared to select the best output of anyone.

Validation and Comparison

The leave-one-out cross-validation is a commonly applied method in Geostatistics because no reserved data are required for the data validation (Benavides et al., 2007). The number of sampled sites with climatic data is usually not very large and they are sparse throughout the study area, so all the sampled data are used for the spatial prediction in order to improve the precision of the predictions (Benavides et al., 2007). In this regards, results were compared by goodness-of fit statistics such as Mean Error (ME), Root Mean Square Error (RMSE), Mean Standardized Error (MSE), Average Standard Error (ASE) and Root Mean Square Standardized Error (RMSSE) (ArcGIS Help, 2014; Benavides et al., 2007; Chen et al., 2013; Delbari et al., 2013; Meng et al., 2013; Wang, Liu, Zhang and Wu, 2011).

$$ME = \frac{1}{n}\sum_{i=1}^{n}[Z(x_i) - Z'(x_i)] \quad (4)$$

$$RMSE = \sqrt{\frac{1}{n}\sum_{i=1}^{n}[Z\ (x_i) - Z'(x_i)]^2} \quad (5)$$

$$MSE = \frac{\sum_{i=1}^{n}[Z(x_i) - Z'(x_i)]/\sigma(x_i)}{n} \quad (6)$$

$$ASE = \sqrt{\frac{1}{n}\sum_{i=1}^{n}[Z'(x_i) - \sum_{i=1}^{n} Z'(x_i)/n]^2} \quad (7)$$

$$RMSSE = \frac{1}{n}\sum_{i=1}^{n}[Z_1(x_i) - Z_2(x_i)]^{\ 2} \quad (8)$$

Where $Z\ (x_i)$ is the measured value of the sample points, and its fitted values are $Z'(x_i)$; Standard values of them are $Z_1(x_i)$ and $Z_2(x_i)$ respectively, and $\sigma(x_i)$ is standard deviation (ArcGIS Help, 2014; Kalivas et al., 2013; Wang et al., 2011).

The ME measures the bias of the prediction and should be close to zero for unbiased methods. It indicates whether the model is, on average, producing estimates that are overestimating or underestimating the observed values. In a well-adapted model, ME and SME should be close to zero for unbiased methods. The RMSE measures the average precision of the prediction and should be as small as possible. The model that performs the best will be the one with the smallest RMSE. This would suggest that the predictions are impartial and close to the respective real values. The values of ASE are used in order to evaluate the prediction divergence from real values. Therefore, ASE should be the same as RMSE, in order to evaluate the divergence of predictions correctly. If the value of the ASE is greater than that of the RMSE this suggests that the variability of the predictions is overestimated. Conversely, if the RMSE is greater than the ASE the variability of the predictions is underestimated. The values of RMSSE should be close to 1. If the RMSSE are greater than 1, then the variability of the predictions is underestimated; if the RMSSE are less than 1, the variability of the predictions is overestimated (ArcGIS Help 2014; Kalivas et al., 2013; Wang et al., 2011).

The ME, RMSE, ASE, SME and RMSSE were calculated to check the performance of each state of interpolations. Therefore, results based on above described rules were compared.

Image Processing: Snow Cover Mapping

Methods for snow-cover mapping can be categorized into three types: manual interpretation, classification-based, and index-based methods (Yin, Cao, Chen, Shao and Chen, 2013). Manual-based methods are the most accurate; however, they are difficult and time-consuming to perform and require the skills of experienced specialists (Yin et al., 2013). Index-based methods, where the normalized difference snow index (NDSI) is frequently used, take advantage of the spectral feature of snow cover characterized as strong reflection in visible/near-infrared wavelengths and nearly total absorption of middle-infrared wavelengths (Crawford, Manson, Bauer, and Hall, 2013; Dozier, 1989; Hancock, Baxter, Evans and Huntley, 2013; Riggs, Hall and Salomonson, 1994; Yin et al., 2013).

In this regard, to map the snow cover area, we followed some steps like spectral characteristics and bands combination to better visualize snow cover and calculate NDSI to combine the manual interpretation and index-based methods.

Spectral Characteristics and Bands Combinations

According to Erdenetuya, Khishigsuren, Davaa, and Otgontugs, (2006) and Bakr, Weindorf, Bahnassy, Marei, and El-Badawi, (2010), to recognize snowy areas with regards to snow spectral characteristics, band combination was used and snow affected regions were extracted in 4,3,2 and 3,2,1 and 5,4,3 combinations as showed in Fig 4 and 5.

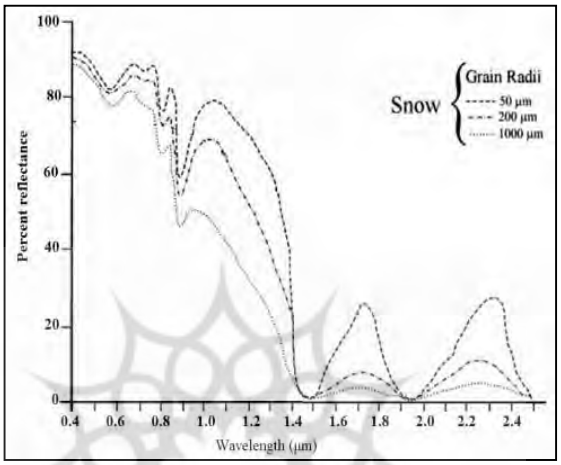

Fig. 4. Snow spectral reflectance. Snow shows variation in spectral reflectance according to the size of crystals in μ (Farooq, 2015).

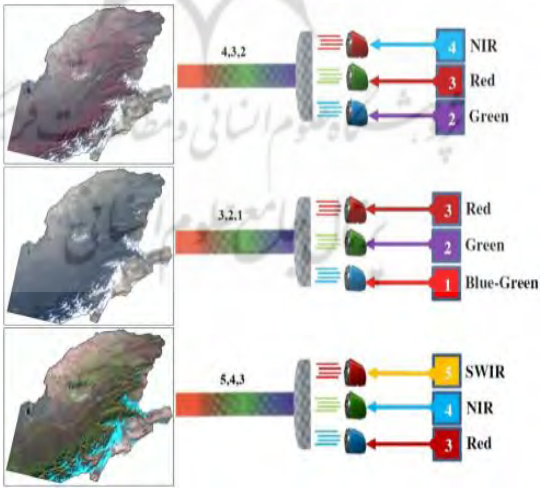

Fig. 5. Landsat band combination to show snow cover (Erdenetuya et al., 2006).

NDSI

As indicated above, the NDSI is the ratio of the difference between reflectance in the infra-red and the visible bands to the sum of the two, to estimate the fractional snow cover (Crawford et al., 2013; Dozier, 1989; Hancock et al., 2013; Riggs et al., 1994). In order to distinguish snow from similarly bright soil, rock and cloud we have calculated NDSI using the following formulae:

$$NDSI = ((Band2 - Band5)/(Band2 + band5)) \quad (9)$$

Where: Band2 and Band5 are Landsat band data (Crawford et al., 2013; Dozier, 1989; Erdenetuya et al., 2006; Klein and Isacks, 1999; Riggs et al., 1994; Wolter, Berkley, Peckham, Singh, and Townsend, 2012).

Results and Discussion

To investigate impact of snow cover extent in images on Geostatistical modeling of air temperature, the area of snow covered regions were extracted from satellite images. The areas of snow cover in each image are presented in Table 2. As can be seen, the greatest area was in December 13, 1986 with around 3800 Km^2, and December 9, 1999 image with less than 400 Km^2 had the smallest SCA.

Table 2. Snow covered area in each image

Sensor / Acquisition date	Snow cover area (Km^2)
TM / 1986.12.13	3786.9
TM / 1986.12.29	1003
TM / 1999.12.01	1261.4
ETM+ / 1999.12.09	367.2

Fig 6 shows some of the predicted maps with the most accurate results. The maps reveal that thermal images have significant impacts and patterns on the interpolation results. Generally, cold temperature spreads in the east of the region including highlands and the warm air temperature is in the interior and somehow north-west (plains). Moreover, a very significant point is that using thermal satellite bands as auxiliary data enhances the spatial quality of the interpolation as presented in details in Fig 6 E-H sections. Section E shows the impacts of topography on local air temperature interpolation. F presents the impact of land cover in interpolation and presents the context of climatic neighborhood of earth features. G shows the impact of the slope aspect on the interpolation of temperature as the south aspects are warmer. And finally in the section, H, the water bodies impacts on the local air temperature are clearly presented. That is why in normal interpolation of air temperature deriving this information is approximately impossible and in case of using other auxiliary data several of them (DEM, Land cover, and so on) are needed to provide these results.

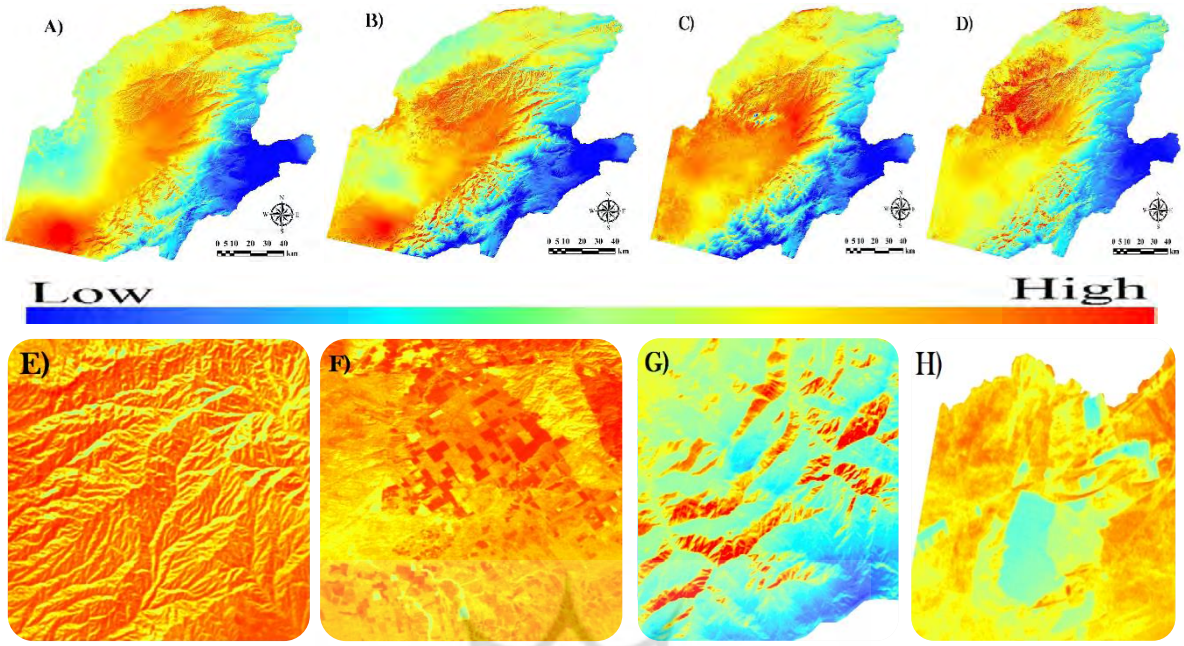

Fig. 6. Some of the air temperature interpolated maps for 1986 and 1999 cold seasons. A) Standard error maps for TCK1986 with more snow covered image. B) TCK1986 with low snow cover image. C) 1999 interpolation with more snow affected image and D) TCk1999 with second satellite image. E) Topographic impact, F) Land cover impact, G) Slope aspect impact and E) water bodies' impacts on air temperature interpolation.

Evaluation and comparing goodness-of fit statistics in Table 3 shows the difference between Thermal Co-Kriging (TCK) outputs based on snow cover area.

Table 3. Results of ME, RMSE, MSE, RMSSE and ASE.

Geostatistics Method	TCK1986-1	TCK1986-2	TCK1999-1	TCK1999-2
Best ME				
ME	0.00	0.00	-0.01	-0.01
RMSE	1.50	1.20	2.80	2.03
MSE	0.05	0.01	0.12	0.10
RMSSE	0.70	0.64	0.90	0.50
ASE	-0.30	-0.40	0.15	-1.70
Best RMSE				
ME	-0.16	0.23	-0.60	-0.60
RMSE	0.78	0.82	1.30	1.30
MSE	-0.05	-0.52	-0.48	-0.48
RMSSE	1.70	3.01	1.94	1.94
ASE	-0.03	0.40	0.41	0.41
Best MSE				
ME	-0.28	-0.11	-0.35	-0.14
RMSE	2.70	1.36	2.80	2.33

Table 3.

Geostatistics Method	TCK1986-1	TCK1986-2	TCK1999-1	TCK1999-2
MSE	-0.01	0.00	0.00	0.00
RMSSE	0.85	0.56	0.89	0.74
ASE	-0.08	-0.60	0.50	-0.38
Best RMSSE				
ME	0.41	-0.35	-0.80	-0.69
RMSE	2.82	0.97	3.20	2.38
MSE	-0.02	0.16	-0.10	-0.13
RMSSE	0.87	0.98	1.00	1.01
ASE	-0.04	0.00	0.50	0.29
Best ASE				
ME	-0.21	-0.35	-0.20	-0.62
RMSE	1.80	0.97	2.70	2.31
MSE	0.01	0.16	0.01	-0.13
RMSSE	0.79	0.98	0.86	0.79
ASE	-0.02	0.00	-0.01	0.01

As mentioned before for optimality and validity of the models if the root-mean-squared prediction error is smaller for a particular model therefore it is the optimal model (ArcGIS Help, 2014). However, when comparing with another model, the root-mean-squared prediction error may be closer to the average estimated prediction standard error (ArcGIS Help, 2014). This is a more valid model because when we predict at a point without data, we only have the estimated standard errors to assess our uncertainty of that prediction. We also must check that the root-mean-square standardized is close to one (ArcGIS Help, 2014). In light of these considerations and as can be understood from Table 3, in spatial interpolation of 1986 the best-unbiased output is belonging to TCK1986-2 but the most accurate is TCK1986-1. TCK with less snow-affected image in 1986 provides precise standard error, too. On the other hand, in 1999 TCK1999-1 shows better results in amount of bias while accuracy with other TCK is the same. In addition, the TCK1999-1 provides more accurate standard error. Totally, comparing the results reveal that in Geostatistical modeling of December 1986 the TCK with more snow cover area had the best ME, RMSE and MSE; conversely, interpolations used less snow covered image had best RMSSE and ASE. For 1999 interpolation, TCK1999-1 is better for ME, MSE, RMSSE and is similar to 1999-2 in RMSE and ASE. Furthermore, if we decided based on RMSE and other statistics in one image, TCK1986-1 is the best for year 1986 and for 1999, the results are similar.

Conclusions

Developing remote sensing data (including thermal bands) is taking place at an unprecedented rate nowadays. In line with this development, satellite images can be relatively easily in access. Thus, we decided to use the thermal bands of the TM and ETM+ sensors as auxiliary data to enhance the mean temperature interpolation quality in the complex regions with less meteorological stations and evaluate the impact of snow-covered area in thermal images on air temperature interpolation. Results revealed that TCK for December 1986 provides better results with more snow affected thermal image.

While in 1999 different results were obtained, the best selected output did not show impacts of different snow cover areas. It should be recalled that in 1999, the snow cover areas are 1261.4 km^2 and 367.2 km^2 and they did not show difference in predicted results. While in 1986 first SCA is 3786.9 km^2 and second one is 1003 km^2. Therefore, it could be conclude that, perhaps 3000 km^2 is the impact threshold.

The future direction of this research includes testing and use of different spatial interpolations, Geostatistics methods, and thermal bands for different regions and time periods. It is recommended to provide thermal inputs of Geostatistics methods using different sampling methods to reduce the volume of calculations. Furthermore, checking the usefulness of the method for other geographical factors that need to be interpolated is important. It is worth noting that this study could open a new window to the climatic neighborhood concept using future studies. In the end, it should be mentioned that it is clear that the number of observation stations are too low and considering the kriging requirements like normal distribution and stationarity is toilsome but this problem exists in many regions in the world and the potential of geostatistics should be considered to solve it.

References

Alsamamra, H., Ruiz-Arias, J. A., Pozo-Vazquez, D., & Tovar-Pescador, J. (2009). A comparative study of ordinary and residual kriging techniques for mapping global solar radiation over southern Spain. *Agricultural and Forest Meteorology*, *149*(8), 1343-1357.

ArcGIS Help. (2014). *Fundamentals of panchromatic sharpening.* Retrieved from http://resources.arcgis.com/en/help/main/10.1/index.html#//009t000000mw000000

Arundel, S. T. (2005). Using spatial models to establish climatic limiters of plant species' distributions. *Ecological Modelling*, *182*(2), 159-181.

Attorre, F., Alfo, M., De Sanctis, M., Francesconi, F., & Bruno, F. (2007). Comparison of interpolation methods for mapping climatic and bioclimatic variables at regional scale. *International Journal of Climatology*, *27*(13), 1825-1843.

Bakr, N., Weindorf, D. C., Bahnassy, M. H., Marei, S. M., & El-Badawi, M. M. (2010). Monitoring land cover changes in a newly reclaimed area of Egypt using multi-temporal Landsat data. *Applied Geography*, *30*(4), 592-605.

Benavides, R., Montes, F., Rubio, A., & Osoro, K. (2007). Geostatistical modelling of air temperature in a mountainous region of Northern Spain. *Agricultural and Forest Meteorology*, *146*(3-4), 173-188.

Boi, P., Fiori, M., & Canu, S. (2011). High spatial resolution interpolation of monthly temperatures of Sardinia. *Meteorological Applications*, *18*(4), 475-482.

Chen, C. F., Yue, T. X., Dai, H. L., & Tian, M. Y. (2013). The smoothness of HASM. *International Journal of Geographical Information Science*, *27*(8), 1651-1667.

Crawford, C. J., Manson, S. M., Bauer, M. E., & Hall, D. K. (2013). Multitemporal snow cover mapping in mountainous terrain for Landsat climate data record development. *Remote Sensing of Environment*, *135*, 224-233.

Cristobal, J., Ninyerola, M., & Pons, X. (2008). Modeling air temperature through a combination of remote sensing and GIS data. *Journal of Geophysical Research-Atmospheres*, *113*(D13), 1-13.

Delbari, M., Afrasiab, P., & Jahani, S. (2013). Spatial interpolation of monthly and annual rainfall in northeast of Iran. *Meteorology and Atmospheric Physics*, *122*(1-2), 103-113.

Dozier, J. (1989). Spectral signature of Alpine snow cover from the Landsat thematic mapper. *Remote Sensing of Environment*, *28*, 9-22.

Erdenetuya, M., Khishigsuren, P., Davaa, G., & Otgontugs, M. (2006, June). *Glacier change estimation using Landsat TM data*. Paper presented at the ISPRS Tokyo 2006 Symposium Technical Commission VI. Tokyo.

Farooq, A. (2015). *Spectral reflectance of land covers.* Retrieved from http://www.geol-amu.org/notes/m1r-1-8.htm.

Hancock, S., Baxter, R., Evans, J., & Huntley, B. (2013). Evaluating global snow water equivalent products for testing land surface models. *Remote Sensing of Environment*, *128*, 107-117.

Hengl, T., Heuvelink, G. B. M., Tadic, M. P., & Pebesma, E. J. (2012). Spatio-temporal prediction of daily temperatures using time-series of MODIS LST images. *Theoretical and Applied Climatology*, *107*(1-2), 265-277.

Jabot, E., Zin, I., Lebel, T., Gautheron, A., & Obled, C. (2012). Spatial interpolation of sub-daily air temperatures for snow and hydrologic applications in mesoscale Alpine catchments. *Hydrological Processes*, *26*(17), 2618-2630.

Joyce, K. E., Wright, K. C., Samsonov, S. V., & Ambrosia, V. G. (2009). *Remote sensing and the disaster management cycle*. Advances in Geoscience and Remote Sensing, Gary Jedlovec (Ed.). InTech.

Kalivas, D. P., Kollias, V. J., & Apostolidis, E. H. (2013). Evaluation of three spatial interpolation methods to estimate forest volume in the municipal forest of the Greek island Skyros. *Geo-Spatial Information Science*, *16*(2), 100-112.

Klein, A. G., & Isacks, B. L. (1999). Spectral mixture analysis of Landsat thematic mapper images applied to the detection of the transient snowline on tropical Andean glaciers. *Global and Planetary Change*, *22*(1-4), 139-154.

Kyriakidis, P. C., & Goodchild, M. F. (2006). On the prediction error variance of three common spatial interpolation schemes. *International Journal of Geographical Information Science*, *20*(8), 823-855.

Li, X., Cheng, G. D., & Lu, L. (2005). Spatial analysis of air temperature in the Qinghai-Tibet Plateau. *Arctic Antarctic and Alpine Research*, *37*(2), 246-252.

Meng, Q. (2006). Geostatistical prediction and mapping for large area forest inventory using remote sensing data. 2006 *UCGIS Summer Symposium*. www.ucgis.org/summer2006/ studentpapers/Mengqm_July03_2006.pdf

Meng, Q. (2014). Regression kriging versus geographically weighted regression for spatial interpolation. *International Journal of Advanced Remote Sensing and GIS*, *3*(1), 606-615.

Meng, Q., Liu, Z., & Borders, B. E. (2013). Assessment of regression kriging for spatial interpolation - Comparisons of seven GIS interpolation methods. *Cartography and Geographic Information Science*, *40*(1), 28-39.

Minaei, M., & Irannezhad, M. (2016). Spatio-temporal trend analysis of precipitation, temperature, and river discharge in the northeast of Iran in recent decades. *Theoretical and Applied Climatology*, *131*(1-2), 167-179.

Minaei, M., & Kainz, W. (2016). Watershed land cover/land use mapping using remote sensing and data mining in Gorganrood, Iran. *ISPRS International Journal of Geo-Information*, *5*(5), 1-16.

Minaei, M., & Minaei, F. (2017). Geostatistical modeling of air temperature using thermal remote sensing. *Environment and Sustainability, 1*(4), 103-109.

Moteallemi, A., Bina, B., Minaei, M., & Mortezaie, S. (2017). The evaluation of noise pollution at Samen district in Mashhad by means of Geographic Information System (GIS)". *International Journal of Occupational Hygiene*, *9*(4), 31-46.

Oliver, M. A., & Webster, R. (1990). Kriging: A method of interpolation for geographical information systems. *International Journal of Geographical Information Systems*, *4*(3), 313-332.

Prakash, A. (2000, July*). Thermal remote sensing: Concepts, issues and applications*. Paper presented at the ISPRS, Amsterdam. ISPRS Archives ˚ 33 (B1).

Riggs, G. A., Hall, D. K., & Salomonson, V. V. (1994, August). *A snow index for the landsat thematic mapper and moderate resolution imaging spectroradiometer*. Paper presented at the Geoscience and Remote Sensing Symposium, IGARSS 94. Surface and Atmospheric Remote Sensing: Technologies, Data Analysis and Interpretation. International, Pasadena, CA, 1994, pp. 1942-1944 vol.4.

Statistical-Center-of-Iran. (2012). *Iranian population and housing census 2011 - Golestan Province General Results.* Tehran: Statistical Center of Iran.

Stewart, S. B., & Nitschke, C. R. (2017). Improving temperature interpolation using MODIS LST and local topography: A comparison of methods in south east Australia. *International Journal of Climatology, 37*(7), 3098-3110.

USGS. (2013). *What are the band designations for the Landsat satellites?* Retrieved from http://landsat.usgs.gov/band_designations_landsat_satellites.php.

Wang, S., Liu, E., Zhang, H., & Wu, W. (2011, February). *Comparison of spatial interpolation methods for soil available P in a hilly area.* Paper presented at 2011 International Conference on Computer Distributed Control and Intelligent Environmental Monitoring, Changsha.

Wentz, E. A., Peuquet, D. J., & Anderson, S. (2010). An ensemble approach to space˚time interpolation. *International Journal of Geographical Information Science*, *24*(9), 1309-1325.

Wolter, P. T., Berkley, E. A., Peckham, S. D., Singh, A., & Townsend, P. A. (2012). Exploiting tree shadows on snow for estimating forest basal area using Landsat data. *Remote Sensing of Environment, 121*, 69-79.

Yin, D. M., Cao, X., Chen, X. H., Shao, Y. J., & Chen, J. (2013). Comparison of automatic thresholding methods for snow-cover mapping using Landsat TM imagery. *International Journal of Remote Sensing*, *34*(19), 6529-6538.

Zaksek, K., & Schroedter-Homscheidt, M. (2009). Parameterization of air temperature in high temporal and spatial resolution from a combination of the SEVIRI and MODIS instruments. *ISPRS Journal of Photogrammetry and Remote Sensing*, *64*(4), 414-421.

Zheng, X., Zhu, J. J., & Yan, Q. L. (2013). Monthly Air Temperatures over Northern China Estimated by Integrating MODIS Data with GIS Techniques. *Journal of Applied Meteorology and Climatology, 52*(9), 1987-2000.